Supplementary Figure 1

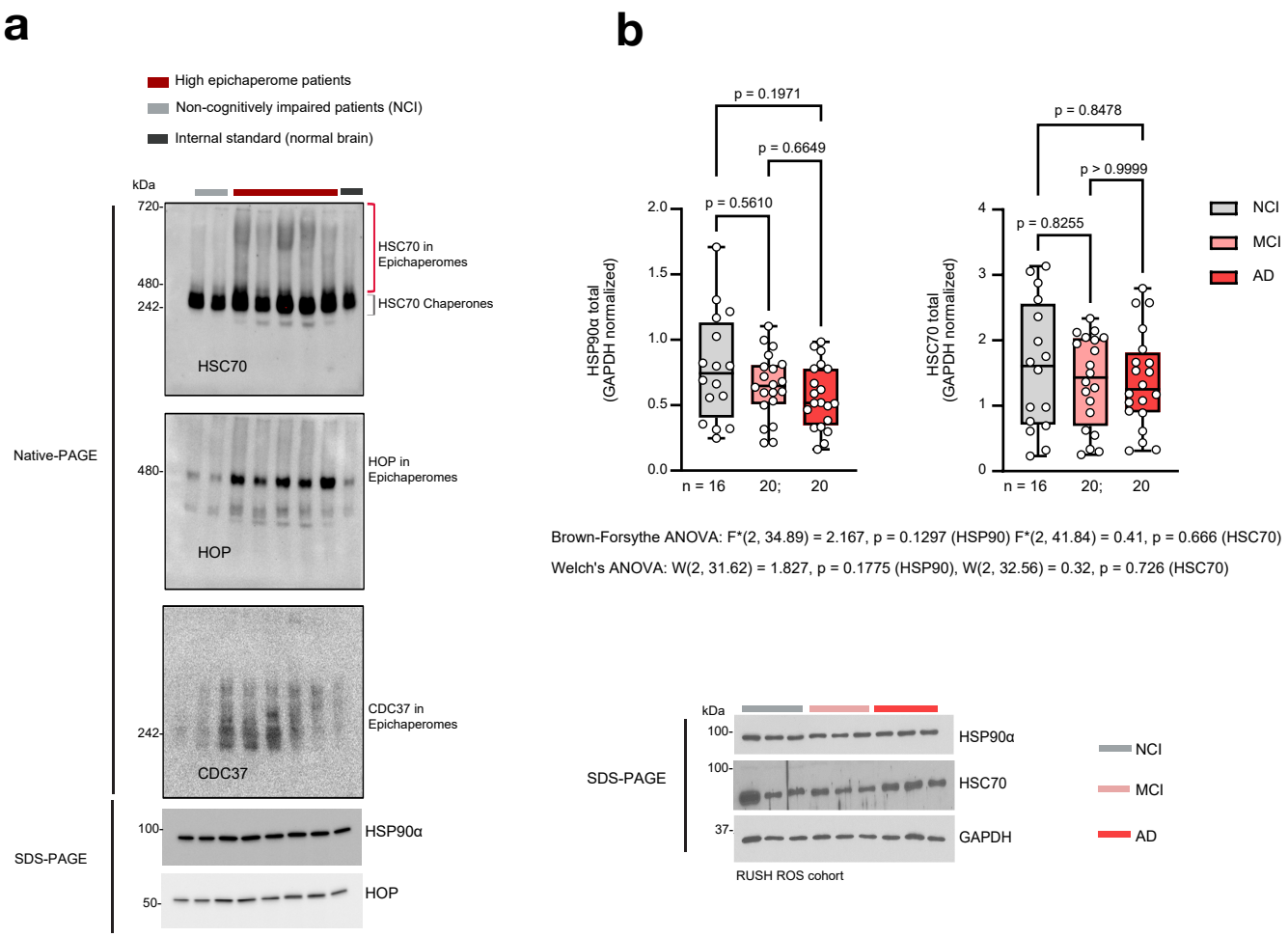

Supplementary Figure 1. Epichaperome formation is independent of chaperone concentration. **a** Epichaperome levels (top) and total chaperone levels (bottom) in high epichaperome patients from the NYU/NKI cohort as evaluated by blotting against epichaperome components HSC70, HOP and CDC37 (top). Gels, representative patients profiles of the n = 108 evaluable samples as in Figure 1. **b** Total chaperone levels within the ROS cohort. Box plots (top) illustrate the distribution of total chaperone levels - HSP90 and HSC70 - across NCI, MCI, and AD cohorts. All data are plotted using a min-to-max box-and-whisker plot, with individual data points representing all values in the dataset. The box indicates the interquartile range, and the line within the box marks the median. The graph was analyzed using Brown-Forsythe and Welch ANOVA with Dunnett's T3 post-hoc test to assess differences among the groups. Both Brown-Forsythe and Welch's ANOVA tests confirm that the total chaperone levels, as represented by HSC70 and HOP, do not significantly differ among NCI, MCI, and AD patients, underscoring that epichaperome formation is independent of the concentration of these chaperones in the evaluated patient groups. Gel (top), representative Western blot analysis of the ROS samples. GAPDH, protein loading control. Source data are provided as a Source Data file.

Supplementary Figure 2

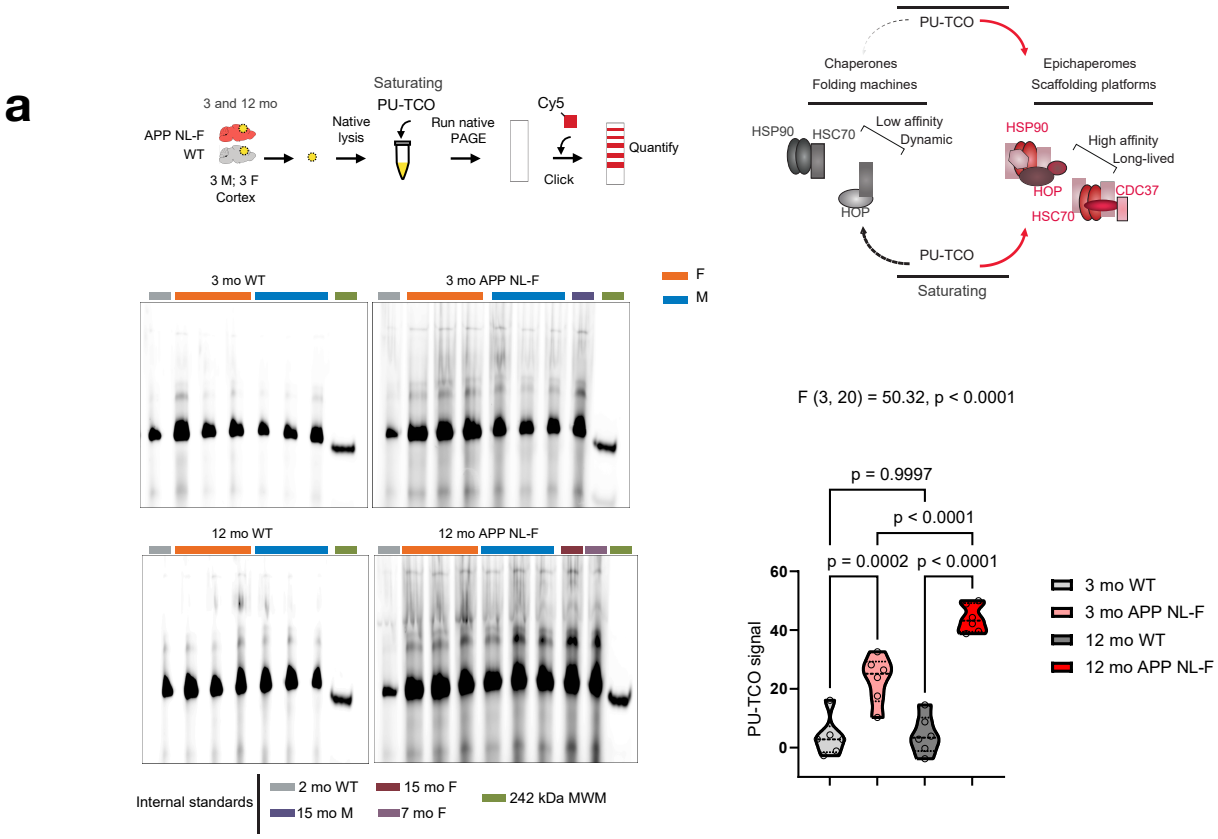

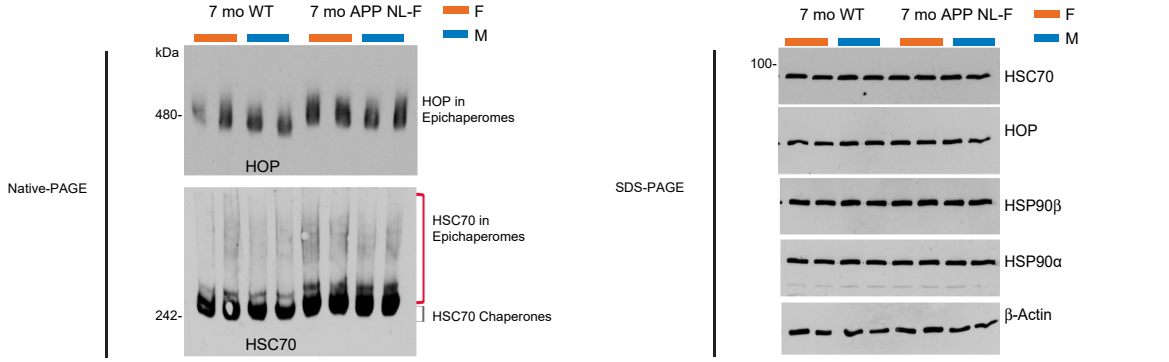

Supplementary Figure 2. Epichaperome formation is preferential in the APP NL-F mouse brain compared to WT and is independent of chaperone concentration.
a Epichaperome and chaperone levels assessed in the cortex of APP NL-F and WT littermates (3 males and 3 females at ages 3 months and 12 months) and detected using the PU-TCO probe clicked to cy5, as depicted in the schematic. Gel micrographs - displaying individual lanes for each mouse -, and truncated violin plots - featuring medians (dotted lines) and quartiles (dashed lines) - illustrate the preferential expression of epichaperomes in the APP NL-F brain. One-way ANOVA with Sidak's post-hoc test was used to assess differences among the groups. **b** Epichaperome levels (left) and total chaperone levels (right) were evaluated in 7-month-old APP NL-F (n = 4) and WT (n = 4) mouse brains (cortex) by blotting for epichaperome components. Gels depict individual lanes for each mouse. Actin is used as a protein loading control. Source data are provided as a Source Data file.

Supplementary Figure 3

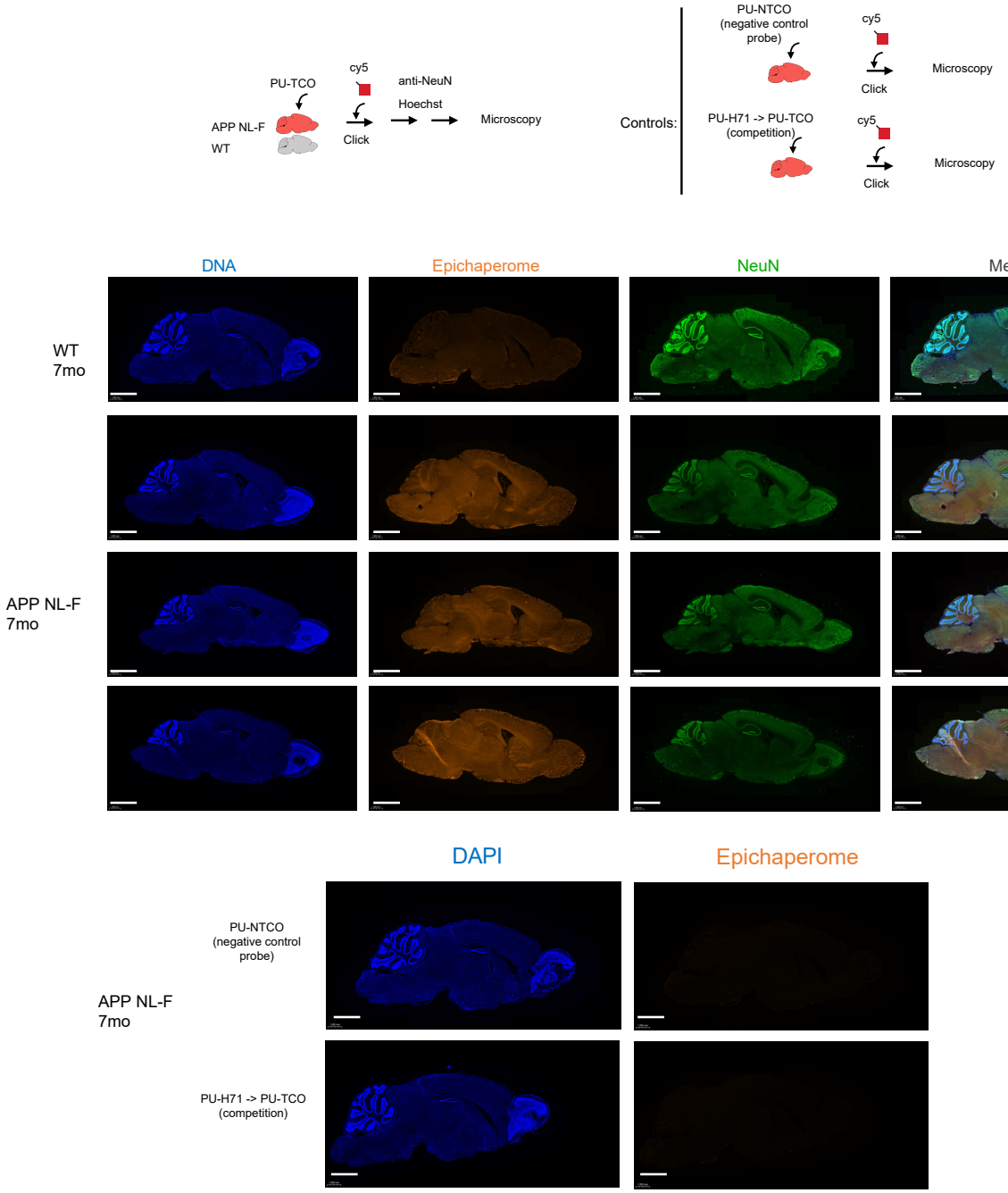

Supplementary Figure 3. Epichaperome detection by PU-TCO in post-mortem murine brains.
Frozen brains harvested from APP NL-F mice (n = 3) and wild-type mice (n = 3) at 7 months of age were sectioned (20 μm) for staining. Sagittal slices were incubated with PU-TCO (1 μM), and then the cy5 fluorescent reporter was attached via click chemistry. Negative controls included PU-NTCO and blocking by pre-treating slices with PU-H71 (1 μM, 1 h) before incubation with the PU-TCO clickable probe. Epichaperomes, orange; Hoechst (blue), for visualization, and staining of cell nuclei. The slides were scanned on a Pannoramic Scanner (3DHistech) using a 20×/0.8NA objective. Scale bars represent 1 mm.

Supplementary Figure 4

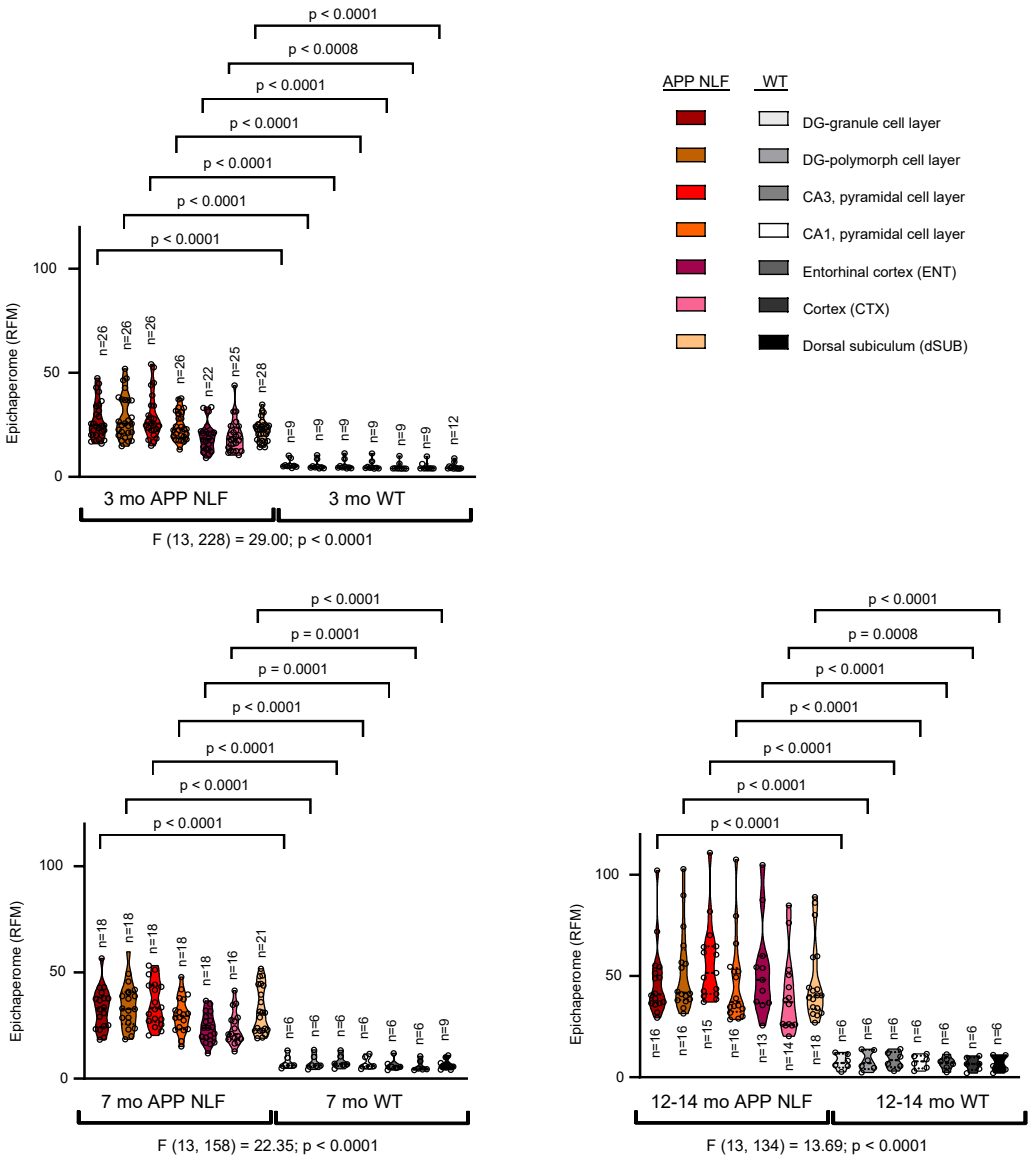

Supplementary Figure 4. Epichaperomes form preferentially in key AD-vulnerable brain regions in APP NL-F mice compared to age-matched WT mice.
a Comparative analysis of epichaperome levels in APP NL-F and WT mice at 3, 7, and 12-14 months of age (3 females and 3 males per group) based on coronal brain slices stained with PU-TCO and clicked to Cy5 dye, corresponding to Bregma -1.22 mm to -2.54 mm (Allen Brain Atlas coronal section images 80-87). Data are plotted using truncated violin plots showing median (dotted line) and quartiles (dashed lines), and analyzed using one-way ANOVA followed by Sidak's post-hoc. All individual data points represent individual brain slice values. Source data are provided as a Source Data file.

Supplementary Figure 5

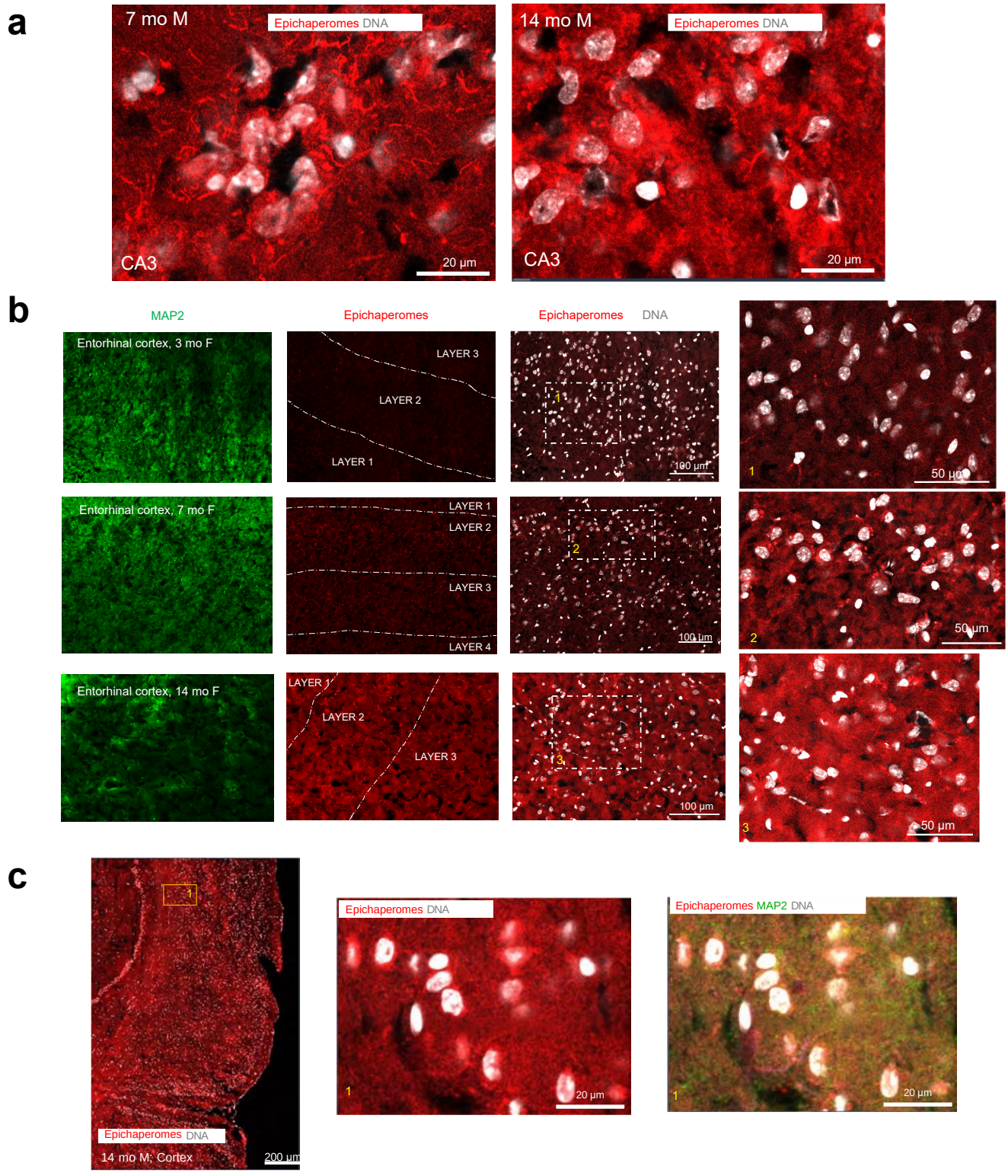

Supplementary Figure 5. Epichaperomes formation in key AD-vulnerable brain cells and regions in APP NL-F mice.
Representative coronal sections from APP NL-F mouse brains (3 female and 3 male mice per age group: 3, 7, and 14 months) as graphed in Figure 4, stained with PU-TCO clicked to Cy5 dye, illustrating epichaperome formation. Images display distinct regions: CA3 (a), entorhinal cortex (b) and cortex (c). Inset for (b), layer 2 neurons of the entorhinal cortex. These neurons are a focal point for early AD pathology, with their vulnerability rooted in their metabolic demands, excitability, and pivotal role in cortical-hippocampal communication. Epichaperomes are shown in red, MAP2 (green) labels neurons, and Hoechst (white/gray) marks nuclei. Scale bar, 20 µm (a); 100 µm (b) and 50 µm inset (b); 200 µm (c) and 20 µm (inset c).

Supplementary Figure 6

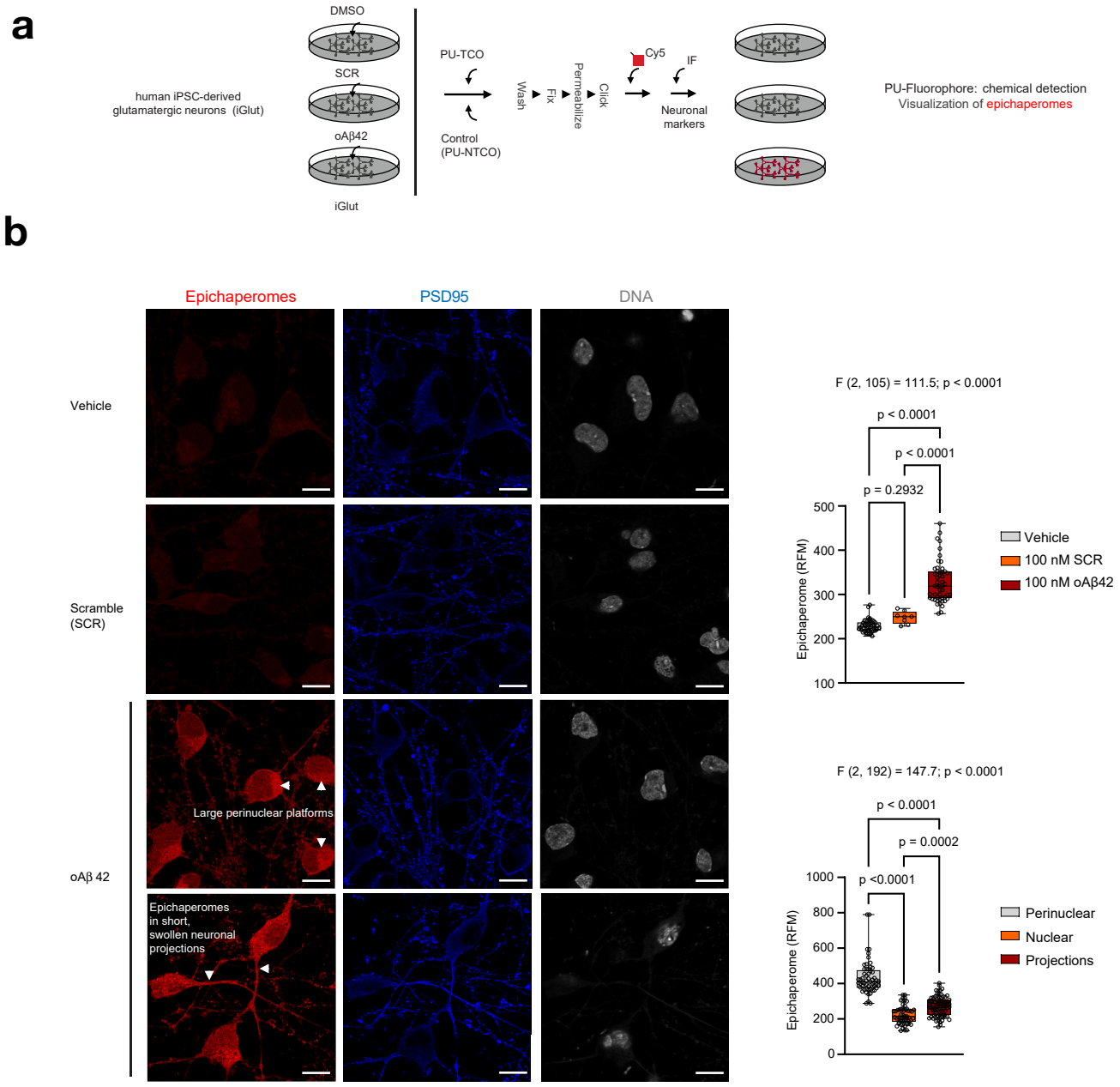

Supplementary Figure 6. Glutamatergic neurons in culture form epichaperomes when exposed to Alzheimer's disease related stressors.
a Experimental Design: The schematic outlines the procedure for treating human iCell Glutatamatergic Neurons (iGlut neurons) with different agents. Confocal microscopic imaging at 63X magnification using Airyscan (Zeiss LSM880) assessed the response of iGluts treated with vehicle control, 100 nM scrambled Aβ42 peptide (SCR), or 100 nM oligomeric Aβ (oAβ42). Stains used: PU-TCO clicked to cy5 for epichaperomes, betaIII tubulin and PSD95 as neuronal markers, and Hoechst for DNA. **b** Representative micrographs (left) and quantitative analysis (right) for each treatment condition (Top: n = 50 Vehicle; n = 8 SCR and n = 50 oAβ42 treated neurons; Bottom: n = 57 perinuclear, n = 57 nuclear and n = 83 projection measurements from n = 57 neurons from three independent experiments). All data are plotted using a min-to-max box-and-whisker plot, with individual data points representing all values in the dataset. The box indicates the interquartile range, and the line within the box marks the median. Data were analyzed using one-way ANOVA with Sidak's post-hoc. Scale bars represent 10 μm. Source data are provided as a Source Data file.

Supplementary Figure 7

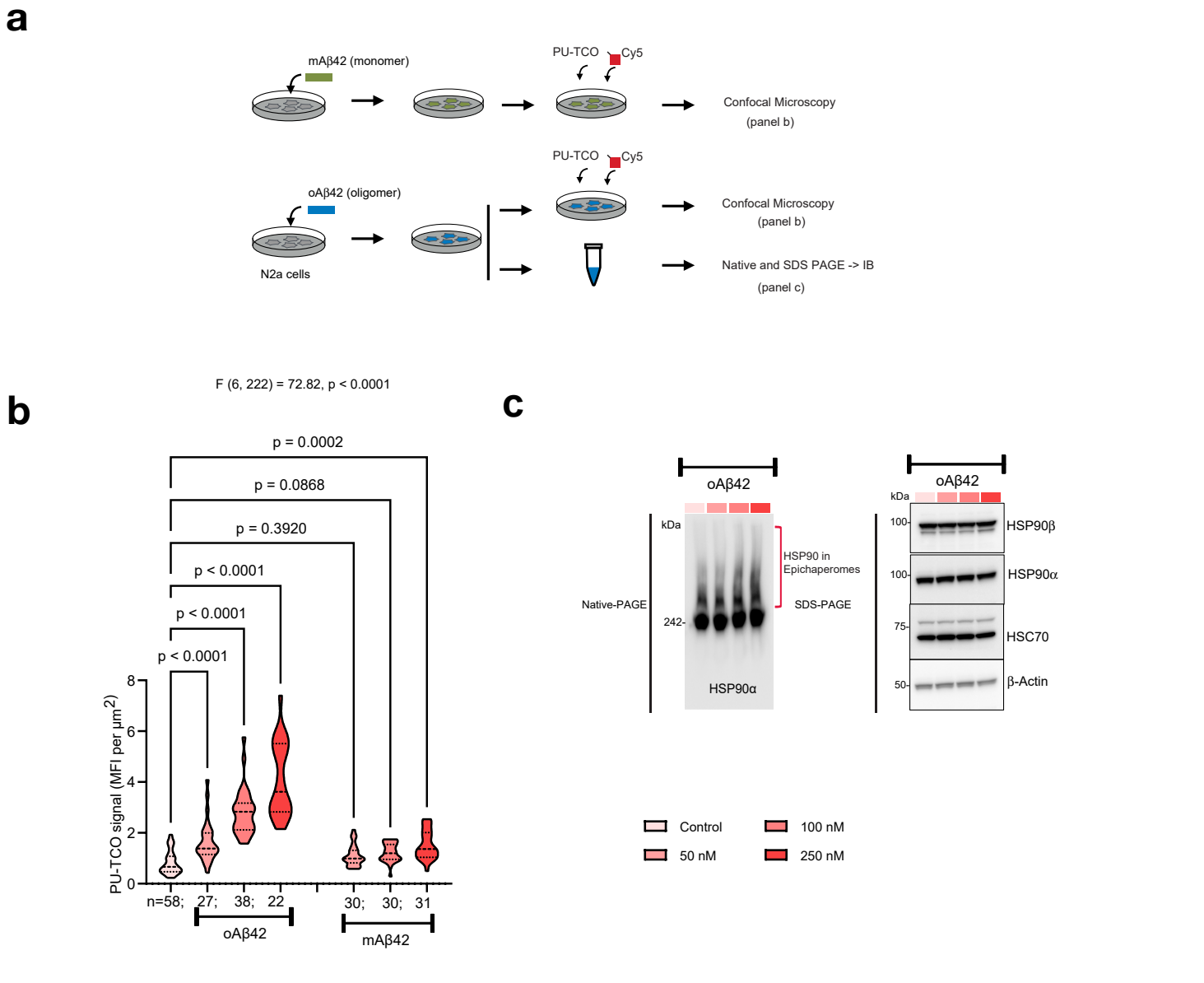

Supplementary Figure 7. Induction of epichaperomes by oligomeric Aβ42 in neuronal cells.
a Experimental schematic. Mouse neuronal (N2a) cells were treated with increasing concentrations of oligomeric Aβ42 (oAβ42) or monomeric Aβ42 (mAβ42) (50, 100, or 250 nM) for 24 hours, alongside a vehicle control. Epichaperome formation was assessed as detailed in the schematic. Note: N2a cells (neuroblastoma) naturally exhibit basal levels of epichaperomes, and these levels are significantly elevated upon treatment with oAβ42 but not with comparable concentrations of mAβ42. **b** Confocal microscopy quantification: Epichaperome presence was quantified using PU-TCO clicked to cy5 staining. Data are represented in truncated violin plots indicating median (dotted line) and quartiles (dashed lines), analyzed using one-way ANOVA followed by Dunnett's post-hoc test. **c** Epichaperome levels (left) and total chaperone levels (right) in N2a cells evaluated after 24-hour exposure to oAβ42, using immunoblotting for specific epichaperome components. Gels depict representative results from replicate experiments. Actin, protein loading control. Source data are provided as a Source Data file.

Supplementary Figure 8

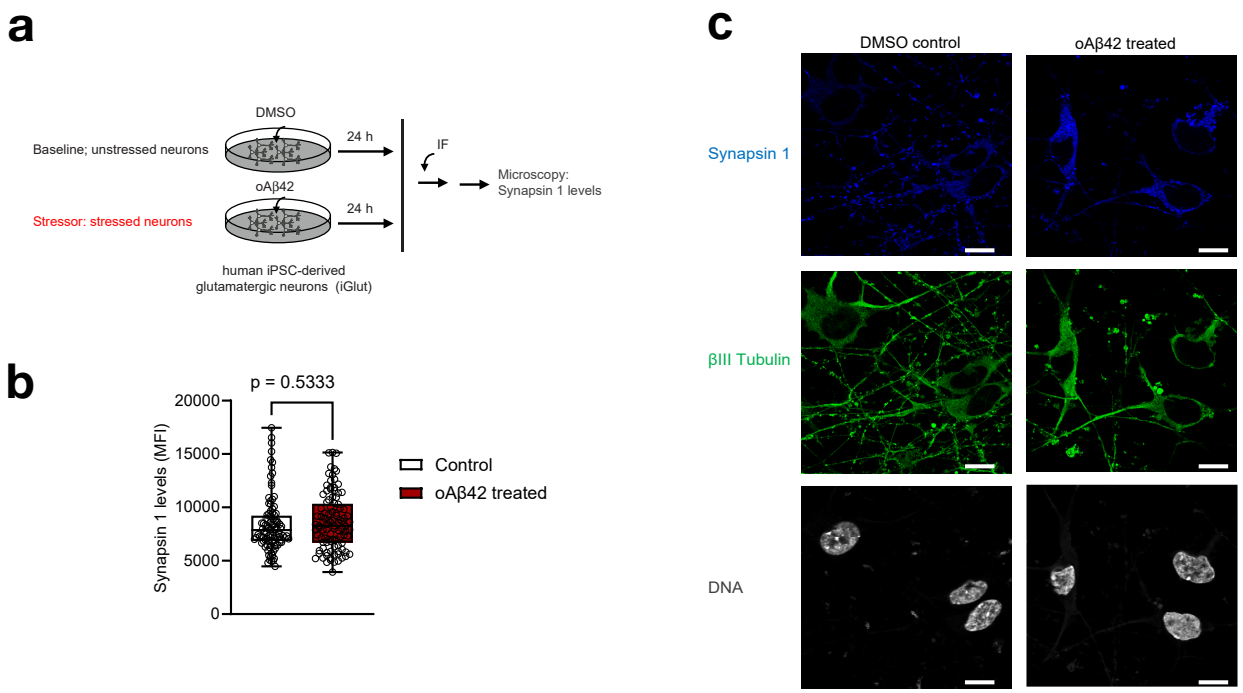

Supplementary Figure 8. Oligomeric Aβ42 alters Synapsin 1 distribution in human glutamatergic neurons without affecting overall levels.
a Experimental design: Confocal imaging (63× magnification, Zeiss LSM880 with Airyscan) was used to assess Synapsin 1 localization in human iCell Glutamatergic Neurons (iGluts) treated with vehicle control or 100 nM oligomeric Aβ42 (oAβ42) for 24 h. Quantification of Synapsin 1 clusters (n = 100 clusters from 20 neurons per condition) determined Synapsin 1 levels and distribution. **b, c** Quantitative analysis (b) and representative micrographs (c) for each treatment condition. Data are plotted as min-to-max box-and-whisker plots, with individual points representing cluster values. Mean fluorescence intensity (MFI) is defined as the average pixel intensity within a selected region of interest (ROI), normalized to the area of the ROI (i.e., cluster). Boxes indicate the interquartile range, and the line within the box marks the median. Statistical significance was determined using an unpaired, two-sided t-test. Control stains: βIII tubulin for neuronal markers and Hoechst for DNA. Scale bars, 10 μm. Source data are provided in the Source Data file.

Supplementary Figure 9

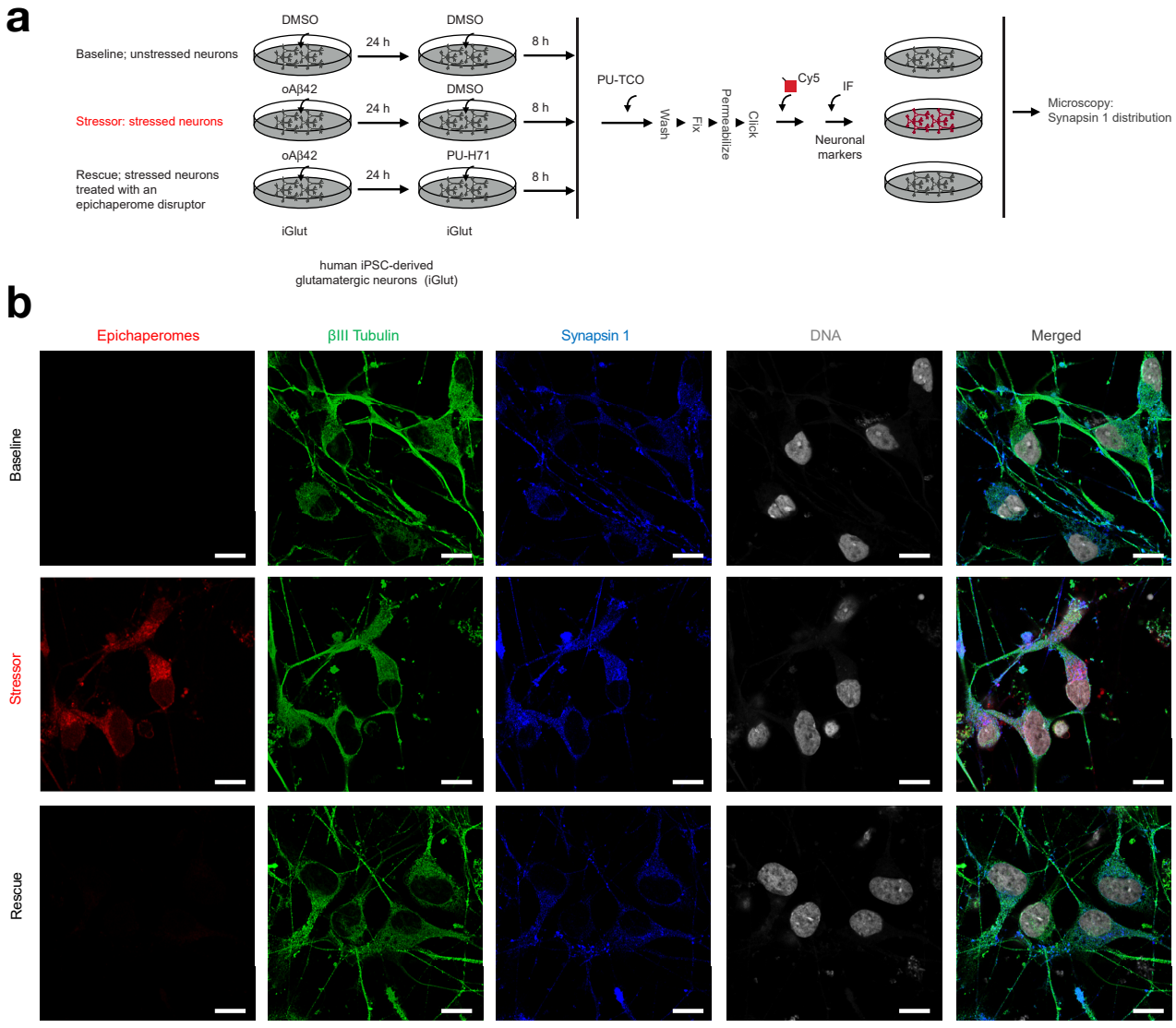

Supplementary Figure 9. Epichaperome disruptors restore Synapsin 1 localization to baseline conditions in oligomeric Aβ42-stressed glutamatergic neurons.
a Schematic representation of the experimental design: Human iCell Glutamatergic Neurons (iGlut neurons) were exposed to an Alzheimer's disease-related stressor (100 nM oligomeric Aβ42, 24 h) followed by treatment with an epichaperome disruptor (1 μM PU-H71, 8 h). The experiment aimed to evaluate the ability of PU-H71 to restore Synapsin 1 localization to pre-stressor conditions. Synapsin 1 levels in the perinuclear region were assessed using confocal microscopy (Zeiss LSM880 with Airyscan) at 63× magnification. **b** Representative micrographs for each experimental condition: Baseline (n = 50 neurons), Stressor (n = 50 neurons), and Rescue (n = 35 neurons), derived from three independent experiments. See also Figure 7d for data quantification and graphical representation. Stains used: PU-TCO clicked to cy5 for epichaperomes, betaIII tubulin as neuronal marker, and Hoechst for DNA. Scale bars represent 10 μm.

Supplementary Figure 10

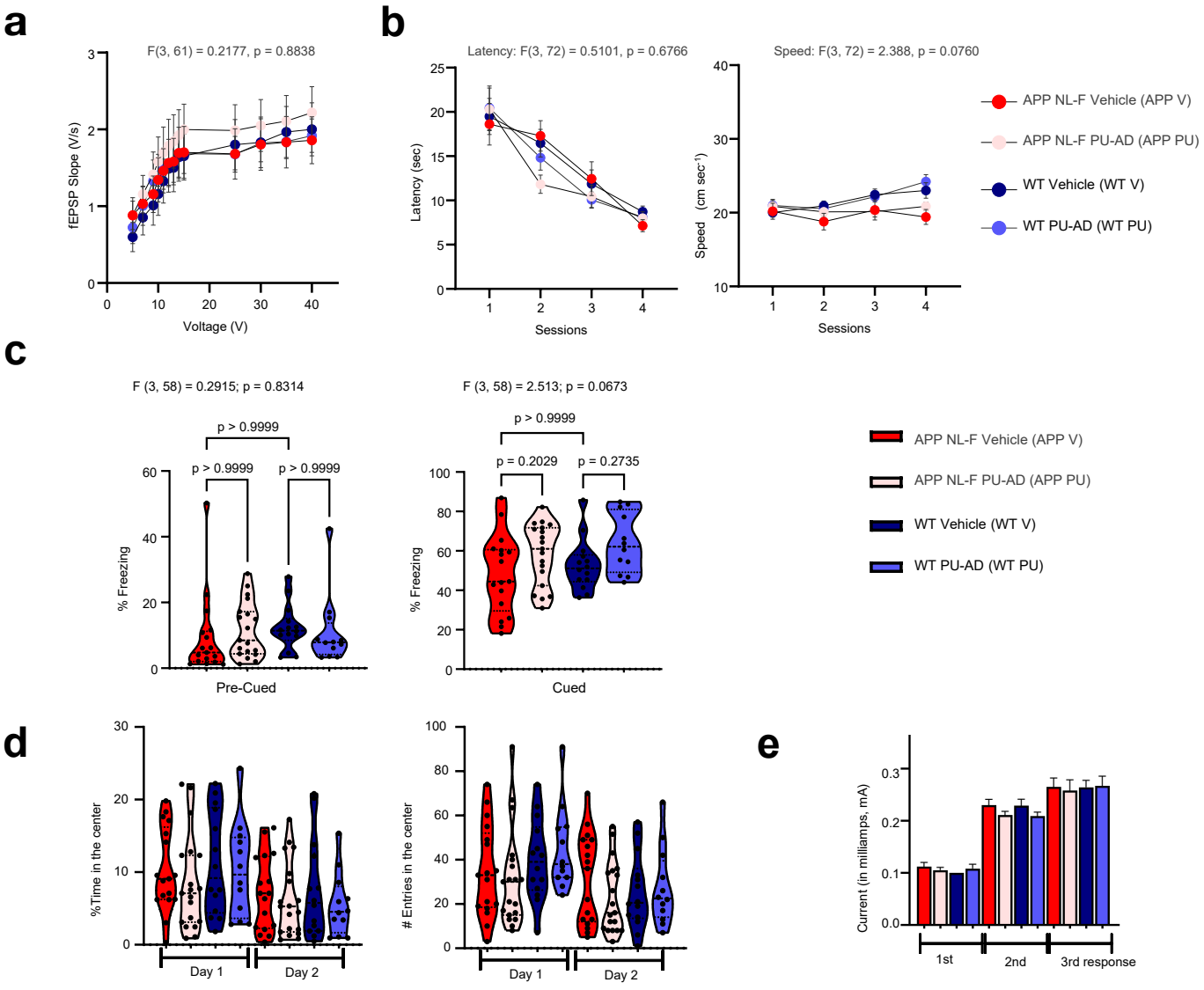

Supplementary Figure 10. PU-AD Treatment Does Not Affect Basal Synaptic Plasticity, Visual-Motor Behavior, Cued Fear Conditioning, Exploratory Behaviour or Sensory Perception in APP NL-F Mice (Prevention Paradigm).
a Basal synaptic plasticity shows no statistical difference across groups. Graph, mean ± s.e.m., two-way repeated measures (RM) ANOVA. n = 15 (3M,5F) for APP V; n = 17 (4M,3F) for APP PU; n = 14 (4M,5F) for WT V; and n = 19 (5M,6F) for WT PU hippocampal slices from individual mice as in Figure 9. **b** Assessment of visual and motor skills evaluated with the visible platform indicate a similar performance related to the average time to reach the platform between the four groups. Graph, mean ± s.e.m., analyzed via two-way RM ANOVA across all groups, n = 19 (10M,9F) for APP V; n = 20 (10M,10F) for APP PU; n = 20 (11M,9F) for WT V; and n = 17 (9M,8F) for WT PU. **c** Cued fear conditioning. Evaluation of the freezing response before and after the presentation of the tone. Mean ± s.e.m., one-way ANOVA with Bonferroni's post-hoc, n = 17 (8M,9F) for APP V; n = 19 (10M,9F) for APP PU; n = 14 (8M,6F) for WT V; and n = 12 (6M,6F) for WT PU. **d** Open field testing showed no difference in the time spent in the center (1-way ANOVA for Day 1: F(3, 58) = 0.5687, p = 0.6378; 1-way ANOVA for Day 2: F(3, 58) = 0.3735, p = 0.7724) and number of entries in the center (1-way ANOVA for Day 1: F(3, 58) = 1.259, p = 0.2967; one-way ANOVA for Day 2: F(3, 58) = 0.7429, p = 0.5309) during both test days across the groups. **e** Sensory threshold assessment (STA) showed no different between the groups for the first visible response (one-way ANOVA: F(3, 58) = 0.6031, p = 0.6156), the first motor response (one-way ANOVA: F(3, 58) = 1.243, p = 0.3024) and the first vocal response (one-way ANOVA: F(3, 58) = 0.04634, p = 0.9866. For open field and STA: APP Vehicle n =17 (8M,9F); APP PU-AD n = 19 (10M,9F); WT V n = 14 (8M,6F); WT PU n = 12 (6M,6F). **a-e** See Figure 9a for experimental design. Source data are provided as Source Data file.

Supplementary Figure 11

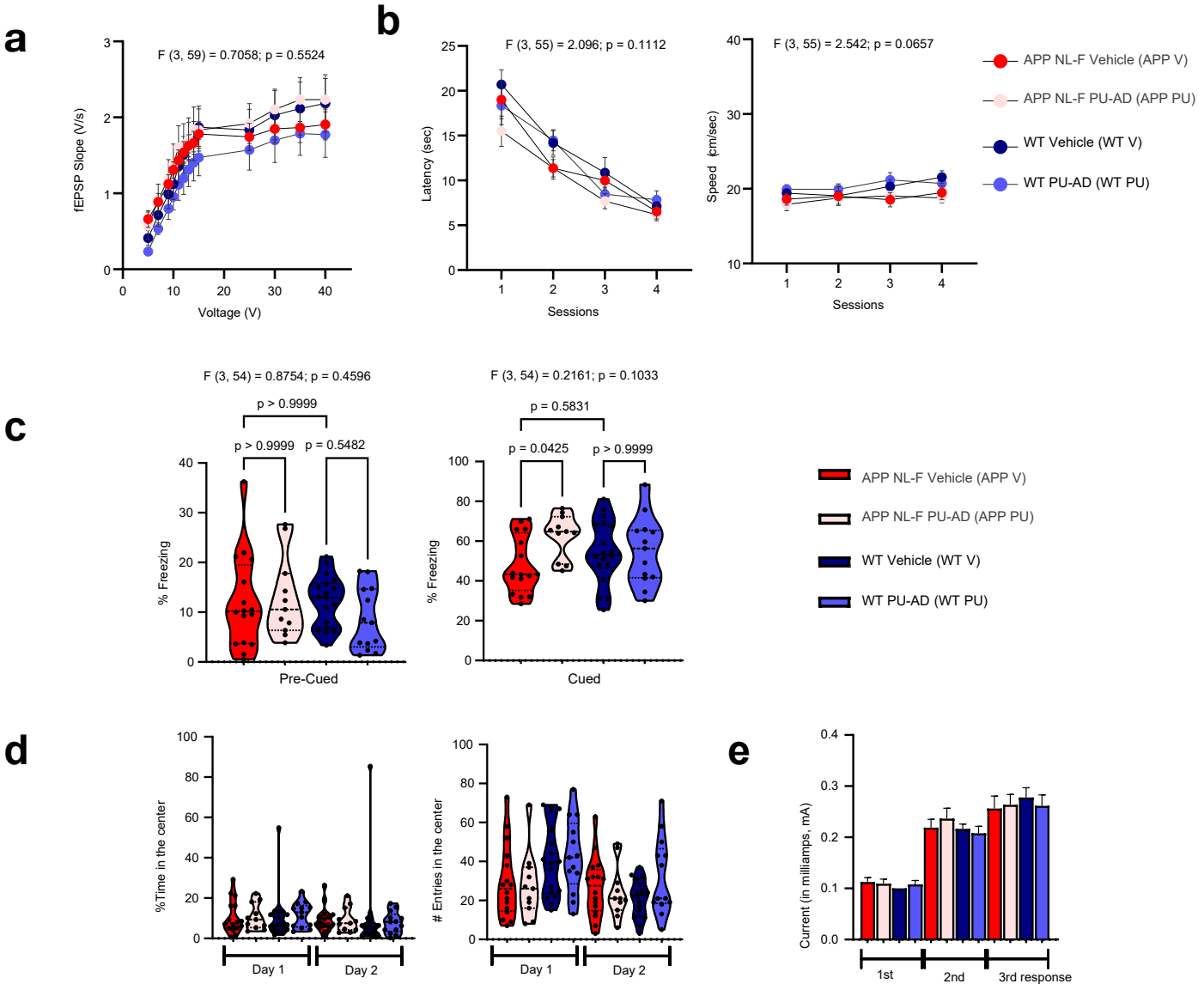

Supplementary Figure 11. PU-AD Treatment Does Not Affect Basal Synaptic Plasticity, Visual-Motor Behavior, Exploratory Behaviour or Sensory Perception in APP NL-F Mice (Reversal Paradigm). **a** Basal synaptic plasticity shows no statistical difference across groups. Graph, mean ± s.e.m., two-way repeated measures (RM) ANOVA of hippocampal slices from individual mice as in Figure 10. n = 16 (4M,5F) for APP V; n = 16 (4M,3F) for APP PU; n = 16 (5M,4F) for WT V; and n = 15 (4M,4F) for WT PU. **b** Assessment of visual and motor skills evaluated with the visible platform as in Figure 10a indicate a similar performance related to the average time to reach the platform between the four groups. Graph, mean ± s.e.m., analyzed via two-way RM ANOVA across all groups, n = 12 (6M,6F) for APP V; n = 12 (7M,5F) for APP PU; n = 17 (8M,9F) for WT V; and n = 18 (9M,9F) for WT PU. **c** Cued fear conditioning. Evaluation of the freezing response before and after the presentation of the tone for mice as in Figure 10a. Mean ± s.e.m., one-way ANOVA with Bonferroni's post-hoc, n = 16 (9M,7F) for APP V; n = 11 (6M,5F) for APP PU; n = 18 (10M,8F) for WT V; and n = 13 (6M,7F) for WT PU. **d** Open field testing assessed general locomotor activity and anxiety-like behavior by measuring time spent in the center and the number of entries into the center of the arena for mice as in Figure 10a. Results showed no significant differences between the groups on both Day 1 ($F(3, 54) = 0.0874$, $p = 0.9667$ for time; $F(3, 54) = 2.351$, $p = 0.0825$ for entries) and Day 2 ($F(3, 54) = 0.0466$, $p = 0.9865$ for time; $F(3, 54) = 1.614$, $p = 0.1969$ for entries). **e** Sensory threshold assessment (STA) for mice as in Figure 10a. The test recorded the visible response (flinching), the motor response (jumping), and the vocal response (vocalization) of mice during increasing foot shock intensity. No differences were observed among the groups for the first visible response (one-way ANOVA: $F(3, 54) = 0.7134$, $p = 0.5483$), the first motor response (one-way ANOVA: $F(3, 54) = 0.5571$, $p = 0.6456$), or the first vocal response (one-way ANOVA: $F(3, 54) = 0.2123$, $p = 0.8875$). Graph, mean ± s.e.m.. For open field and STA: APP Vehicle n =16 (9M,7F); APP PU-AD n = 11 (6M,5F); WT V n = 18 (10M,8F); WT PU n = 13 (6M,7F). Source data are provided as Source Data file.